Evidence for the independent existence of three isomers of protonated ferrocene and their mechanisms of formation

Rod S. Mason* and Lara J. Kelly
Institute of Mass Spectrometry,[#] College of Medicine, Swansea University, Singleton Park, Swansea, SA2 8PP, UK
E-mail: r.s.mason@swansea.ac.uk

This paper is dedicated to Professor Keith Smith, of Cardiff University, and formerly an outstanding Head of the Chemistry Department, Swansea University, on the occasion of his retirement

DOI: http://dx.doi.org/10.3998/ark.5550190.0013.709

Abstract

Gas phase protonation of ferrocene has been studied experimentally in four different reaction systems, using high energy Collision Induced Decomposition mass spectrometry to follow the progress of reaction at different temperatures and pressures. Experimental evidence is obtained for the existence of three stable isomers as predicted theoretically. The most stable form is shown to be most probably metal-protonated, but the energies of the metal-protonated and *agostic* forms are within 10 kJ mol^{-1} of each other. The ring-protonated isomer is higher in energy by $\leq$ 62 kJ mol^{-1}. Intramolecular isomerization could not be detected, indicating relatively high energy or entropy barriers separating the isomers. The intermediate complex formed by *exo* attack of t-$C_4H_9^+$ on ferrocene was also studied and observed to change structure, from a σ- to a π-complex, leading to the population of different protonated isomers of ferrocene, depending on the temperature.

Keywords: Ferrocene protonation, collision induced decomposition mass spectrometry

---

Introduction

The protonation of ferrocene is a fundamental reaction of organometallic chemistry which has been studied extensively over a period of 60 years.[1,2] It is of interest because of the fluxional behaviour of protonated ferrocene in solution[3] and the reaction is a prototype for electrophilic attack. Although it is the simplest electrophilic chemical reaction of ferrocene, there is still a debate concerning (i) the reaction mechanism, (ii) the possible structures of the protonated molecule and (iii) their relative energies. So far, neither clear experimental evidence for the existence of different protonated forms of ferrocene, nor the details of the protonation reaction mechanism, have been obtained.[4] The different possible theoretical structures[4,5] of protonated ferrocene have the proton attached directly onto the metal (**1a**), or to both the iron atom and the underside of one of the cyclopentadienyl rings (**1b**), or attached to one of the rings, **1c**, as shown in Figure 1. The **1b** isomer is often referred to in the literature as the "agostic" form of the isomer, a term that is also adopted here.

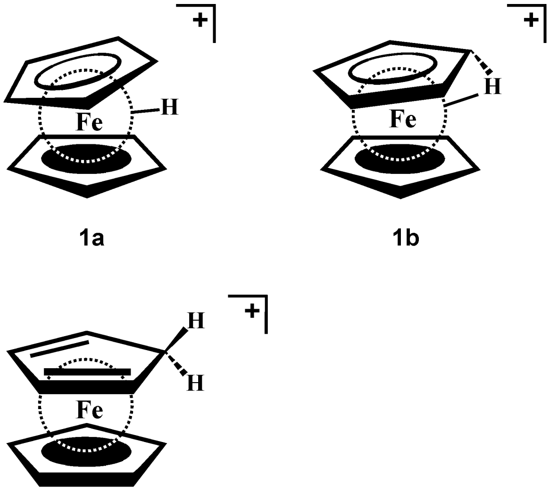

1a **1b** **1c**

Figure 1. Theoretical structures of the isomers of protonated ferrocene.

In proton exchange, the donated proton always comes attached to a Brønsted acid and will be transferred in the intermediate ion-molecule complex, to either ring or metal, depending on the structure of the complex and the energetics of the processes involved. Experimental evidence, in the form of products of reactions carried out in solution, points to both ring and metal protonation. Isotopic scrambling in the deuterated molecule has been interpreted as being caused by initial *exo*[6] attack on one of the cyclopentadienyl rings, which is followed by intramolecular transfer across to the other, via intramolecular protonation of the metal atom. On the other hand, in superacid at low temperature, primary protonation occurs[7] via the *endo*[6] approach directly onto the metal, or to form the agostic structure. In general, in the language of physical organic chemistry, it has been suggested[8] that 'strong' electrophiles would favour *exo* attack to form the σ-complex, whilst 'soft' electrophiles would favour the *endo* route.

Protonated ferrocene has already been studied quite extensively in the gas phase.[9–12] Fundamentally this approach avoids the solvent effect, giving results that are more directly comparable to theoretical calculations. The proton affinity (P_A) was measured[9,12] previously to be in the region of 864 kJ mol^{-1}, and it was inferred that the proton attaches to the iron atom.[9,10,12] In the reaction with D_3O^+ the integrity of the exchanged D^+ seems to be retained without significant scrambling, from which it was suggested[9] that the exchanged proton is uniquely sited on the molecule and does not readily exchange with the H atoms of the ring.

Exothermic ion-molecule reactions in the gas phase often proceed at close to the collision capture rate (which is large because of the ion-polar and ion-dipolar interactions), with little temperature dependence. Exceptions occur when there is significant steric hindrance, also causing a negative temperature dependence, which is true of some reactions involving proton transfer to ferrocene.[9,12] In one case (the transfer from protonated acetophenone,[13] P_A = 861 kJ mol^{-1}) Kebarle *et al*.[12] found that the temperature dependence changed from negative to positive above 420 K. It was suggested that this could be a change at higher temperature to an endoergic protonation channel, to a site about 40 kJ mol^{-1} higher in proton affinity than the metal atom, i.e. one of the cyclopentadienyl rings.

Attempts to calculate the energies and structures of protonated ferrocene by molecular orbital (MO) theory calculations have yielded mixed results.[4,5,14-16] At the MP2/6-311G level of MO theory the ring-protonated form is 176 kJ mol^{-1} higher in energy than the metal-protonated version.[5] Density functional theory (DFT) calculations at the BPW91/6-311G level of theory predict the metal-protonated and agostic forms to be close in energy.[16] Coupled-cluster calculations[4] give a theoretical proton affinity of ferrocene which is close to the experimental value, predicting the agostic form to be the more stable by 11 kJ mol^{-1}. This technique failed, however, to yield a minimum energy for the ring-protonated isomer.

In this paper we present the results of an investigation of the gas phase protonation of ferrocene, as a function of temperature and pressure, using high energy collision-induced decomposition (CID) mass spectrometry to monitor the products of reaction. In this technique, selected ions from the relatively high pressure reaction mixture are sampled, accelerated in a vacuum to a very high energy, then passed through a collision gas, which causes fragmentation. The resulting mass spectrum of the product ions of the collision can sometimes distinguish between isomeric ion structures produced in the reaction of interest. Protonated ferrocene, created by chemical ionization in methane, was investigated by McMahon and co-workers[17,18] using both relatively low energy (<10 eV collisions) and very high energy collisional activation (8000 eV collisions). The main CID processes identified were (1) and (2).

$$\textit{CID}: \quad FeCp_2H^+ \rightarrow FeCp_2^+ + H \qquad (\mathbf{1})$$

$$\textit{CID}: \quad FeCp_2H^+ \rightarrow FeCp^+ + C_5H_6 \qquad (\mathbf{2})$$

Deuterated ferrocene, $FeCp_2D^+$, was also studied. A high ratio for loss of H in favour of D in the equivalent of reaction (1) was interpreted[18] as indicative of ring protonation, which was opposite to Meot-Ner's deduction of metal protonation from his kinetic study of the deuteration reaction itself.[9]

The emphasis in our study was the use of various protonating agents with a wide range of reaction exothermicities, under controlled reaction conditions of temperature and pressure. The instrument used was also different, but which has proved useful previously (in favourable systems) in distinguishing protomers, close in structure and energy,[19,20] and following the changes in relative abundance as the proton moves from one site to another[21] as the temperature of the reaction gas is changed. The results of the present study demonstrate the independent existence and mechanism of formation of all three isomers of protonated ferrocene, which give distinctive patterns of behaviour in their CID mass spectra, depending on the reagent used and the reaction conditions. Relative energies have also been estimated.

Results and Discussion

The different reactions studied and the reaction exothermicities are summarized in Table 1.

Table 1. Proton transfer reactions: $\mathbf{B}H^+ + FeCp_2 \rightarrow \mathbf{B} + FeCp_2H^+$, and their reaction exothermicities[a] (ΔH kJ/mol) as studied in this work

Reagent gas[b]	CH_4			C_6D_5F[c] in CH_4	$(CH_3)_2CHCH_3$	NH_3
BH$^+$	CH_5^+	$C_2H_5^+$	$(C_6H_5CH_3)H^+$	$(C_6D_5F)H^+$ [d]	$(CH_3)_3C^+$	NH_4^+
ΔH	–329	–199	–85	–108	–62	–10

[a]Estimated from the differences in proton affinities in reference 13; uncertainties are quoted as 8 kJ mol^{-1}, therefore the uncertainties in ΔH are 11 kJ mol^{-1}, except for the ammonia system which according to ref. 12 is accurate to within 4 kJ mol^{-1}. [b]Reaction mixtures were made up usually as reagent gas : toluene : ferrocene. [c]Ratio ferrocene : perdeuterated fluorobenzene : methane ≈ 1 : 10 : 3333. [d]The product was an approximately equimolar mixture of $FeCp_2H^+$ and $FeCp_2D^+$.

Ions created from the different reaction mixtures are shown in Figure 2. These are in effect ‘Chemical Ionisation Mass Spectra’. Both reagent and product ions appear. In order to study the isomers of protonated ferrocene, the $FeCp_2H^+$ ion from each reaction mixture is selected by setting the mass spectrometer scan conditions and recording the CID mass spectrum.

Kebarle *et al*.[12] reported that, in general, the efficiency of proton transfer to ferrocene slows down as the reaction exothermicity decreases. The reactions studied here were carried out under similar conditions, and it is readily seen from the intensity ratios of $FeCp_2H^+$ and NH_4^+ in Figure 2(c) that the reaction in ammonia is indeed much less efficient than that in the other considerably more exothermic reaction mixtures. It will be shown that if the exothermicity of the reaction is sufficient to attach the proton initially onto an *exo* site, i.e. directly onto the ring, reaction is fast. When the energy available is only enough to place the proton into an *endo* position, however, then steric factors inhibit the reaction.

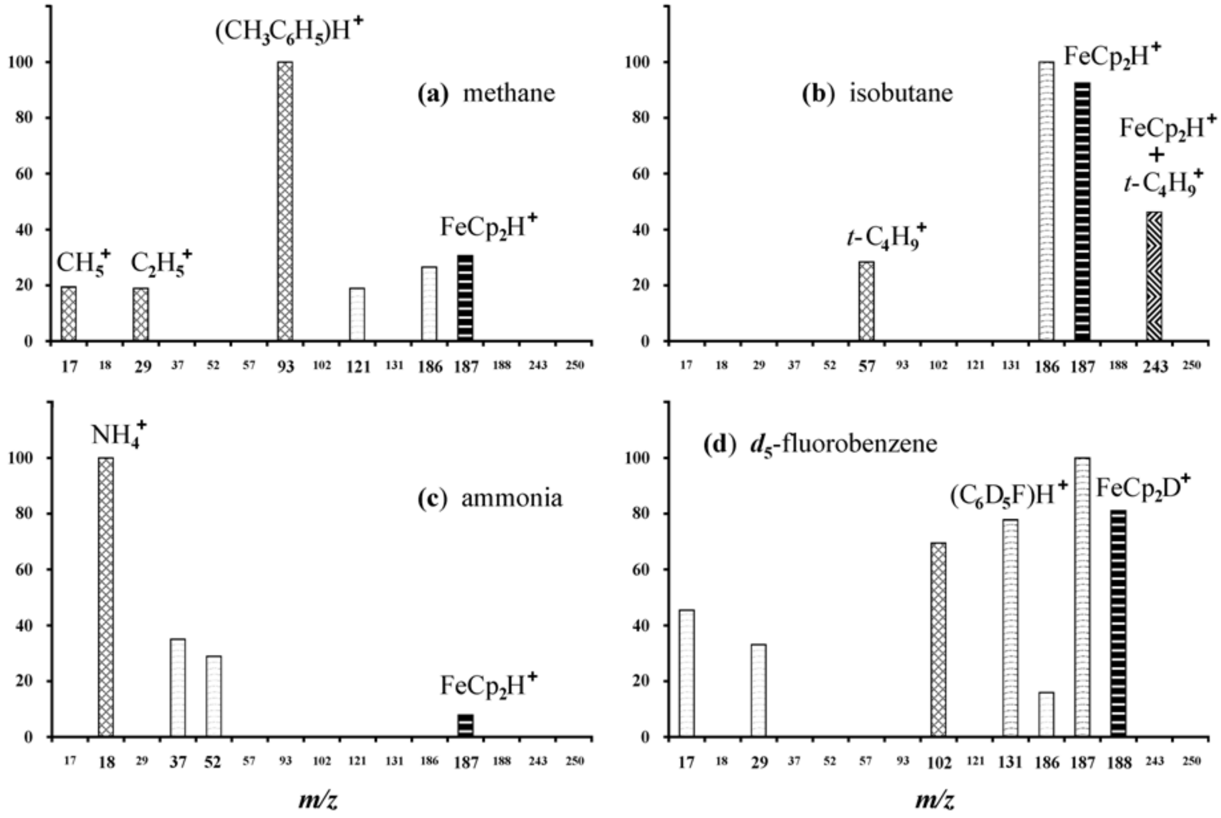

Figure 2. Relative steady state ion abundances in the four gas reaction mixtures studied (pressure: 1 Torr, temperature: 160 ºC) containing ferrocene vs. their *m/z* ratios, showing both reactant and product ions present at ≥ 5% of the most abundant.

High energy CID mass spectrometry

The nature and speed of the interaction in a high energy ion beam collision experiment activates the ions subsequently detected on the timescale of a single vibration, via almost 'vertical' electronic transitions.[22] The energised molecule, therefore, starts off with the geometry of the ground state ion.[23] The energy gained during the high energy collision is transferred from the initial site of activation and is shared with the rest of the molecule. Frequently, this leads to a high flux of energy through single bonds leading to direct bond cleavage before the energy gets randomised throughout the whole molecule. Generally, for a given excitation energy of the parent ion, fragmentations depend on two parameters: (i) the excess of energy in the transition state of the decomposition pathway and (ii) the degree of atomic rearrangement required to reach that transition state. Hence, high energy processes may sometimes dominate lower energy processes if the latter require significant rearrangement. This means that, in favourable systems, even quite subtle differences in structure can lead to significantly different intensity patterns for the fragmentations. In some cases, even changes in rotational energy of the ground state ion can be detected.[22]

CID spectra of $FeCp_2H^+$: pressure and temperature dependence. High energy CID mass spectra (ms) were measured for protonated ferrocene, formed under a range of reaction conditions and prepared using the variety of reagents shown in Table 1. Significant differences were observed depending on the reagent ion used and the temperature of the gas, indicating changes in the isomer population of protonated ferrocene. Examples are shown in Figure 3. The *m/z* ratio of $FeCp_2H^+$ is 187. The CID ms peaks at *m/z* = 186, 129, 121 and 56 are caused by decomposition in which the neutral fragments breaking away from $FeCp_2H^+$ are respectively H, FeH_2, c-C_5H_6 and $C_{10}H_{11}$ by reactions (1) and (2) as used in previous studies, but also reactions (3) and (4).

$$\mathit{CID}: \qquad FeCp_2H^+ \rightarrow C_{10}H_9\rceil^+ \quad + \; FeH_2 \qquad (\mathbf{3})$$

$$\mathit{CID}: \qquad FeCp_2H^+ \rightarrow Fe^+ \quad + \; C_{10}H_{11} \qquad (\mathbf{4})$$

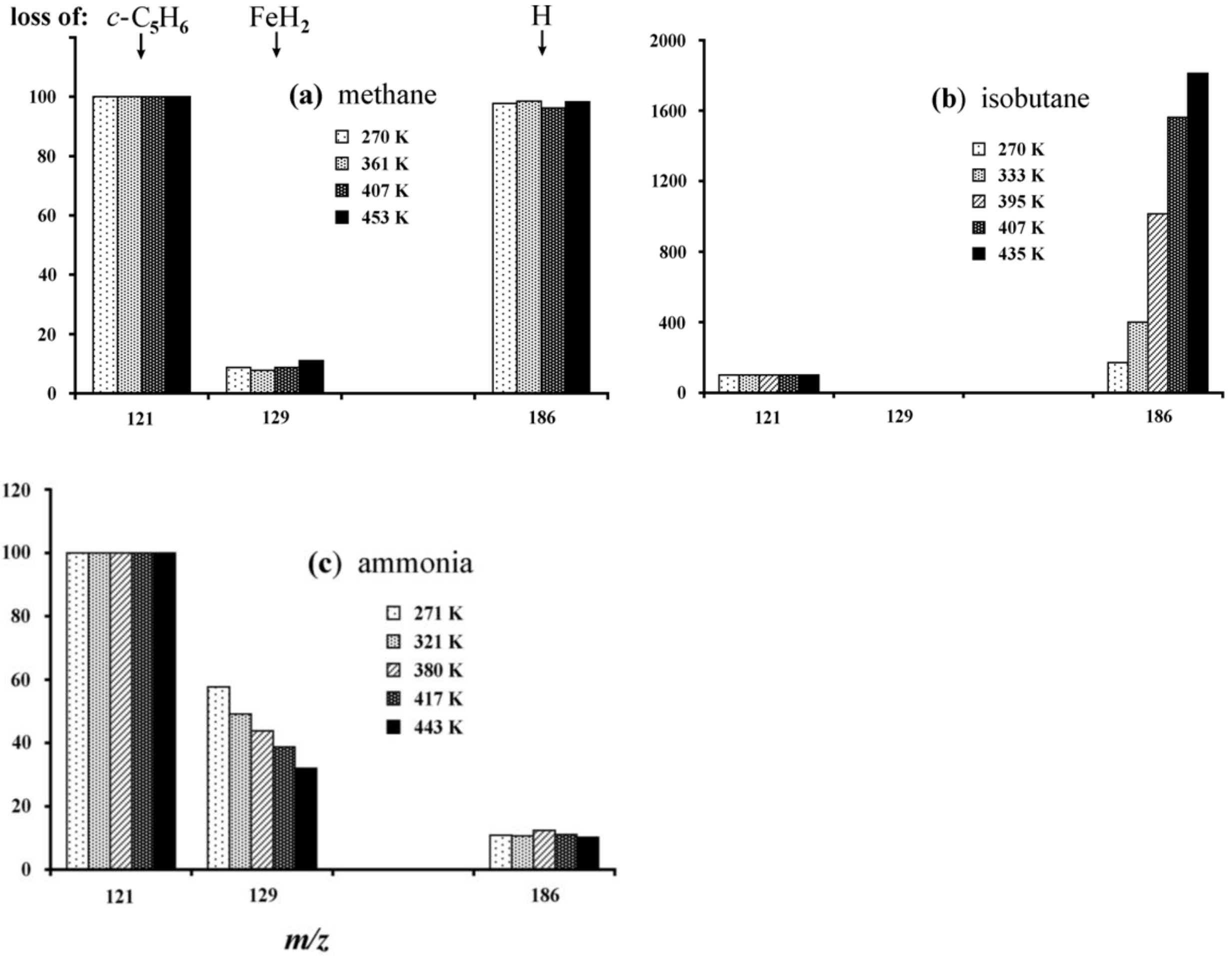

Figure 3. Comparison of CID spectra of $FeCp_2H^+$ obtained for various reagent gases and temperatures. Ion intensities ≥ 5% of the *c*-C_5H_6 loss peak, and normalized with respect to it, are shown at their selected mass to charge ratios.

Losses of H and c-C_5H_6 in reactions (1) and (2) could go via direct bond cleavage, but losses of FeH_2 and $C_{10}H_{11}$ in (3) and (4) both clearly require considerable rearrangement prior to decomposition. The endothermicities are summarized in Table 2. Other peaks of lower relative intensity were observed, as also occurred in the high energy CID study by Hop and McMahon[17] (using a methane gas mixture), but it is the ones listed here which turned out to be significant in structural identification.

The spectra were found to be independent of both partial pressure of ferrocene and the total gas pressure in the reaction cell at all temperatures; an example is shown in Figure 4 for the isobutane system. This also shows up the FeH_2 loss for this system (which on the scale used in Figure 3(b) is insignificant).

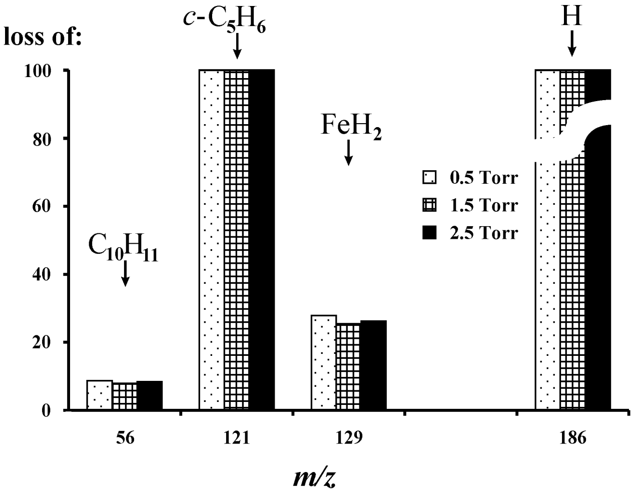

Figure 4. CID spectrum of $FeCp_2H^+$ created in the isobutane gas system as a function of total pressure; reaction conditions were otherwise as for Figure 3(b).

Table 2. Endothermicities[a] of decomposition channels in the high energy CID of protonatedferrocene: parent ion (CID) → fragment ion + neutral loss

m/z of ion in the CID spectrum	Fragment ion	Neutral loss	ΔH (kJ mol^{-1})	Comments
187	$(FeCp_2)H^+$			parent ion
186	$FeCp_2^+$	H	214	
129	$C_{10}H_9^{+\,b}$	FeH_2	> 386[b]	
121	$FeCp^+$	c-C_5H_6	309	

[a]Energies used in these calculations were taken from references 24 and 25. [b]This ion is common in electron impact mass spectra of ferrocene derivatives and is formed by the 'condensation' of the two rings, possibly creating protonated fulvalene or a Diels–Alder reaction product; in the energy calculation, the energy of the much more stable isomer, protonated naphthalene, was used to estimate a lower limit to the endothermicity.

Hop and McMahon[18] studied reactions in methane and in D_2O/CH_4 and *tert*-butyl chloride-*d*$_9$/CH_4 mixtures, although their reaction conditions were not specified. From their data they concluded that CID products of protonated ferrocene are independent of the exothermicity of reaction. Figure 3 shows that in our experiments this is clearly not the case, although the range of reagents and conditions explored here is wider. Furthermore, two of the systems (isobutane and ammonia) displayed pronounced reaction temperature dependences: Figures 3(b) and 3(c). The CID spectrum of $FeCp_2H^+$ formed in methane (Figure 3a) was independent of both reaction temperature and pressure.

The CID spectrum of $FeCp_2H^+$ formed in methane showed high losses of H and *c*-C_5H_6, whilst loss of FeH_2 contributed less than 10%. In the isobutane system at high temperature (435 K) the loss of H peak is very large, the other peaks contributing less than 5%. The H loss peak drops in intensity by a factor >10 when the reaction temperature decreases to 270 K, although it is still dominant over the other peaks. The FeH_2 peak is not shown for the isobutane system in Figure 3(b), but it also drops relative to the *c*-C_5H_6 peak, by a factor just >3. The H loss peak in the ammonia generated spectrum, Figure 3(c), is only 6% of the *c*-C_5H_6 loss, and the ratio of the two remains constant as the temperature is changed. On the other hand, the FeH_2 peak, which has 30% relative abundance at 440 K, increases to 60% as the temperature drops to 270 K.

It is clear from the changes in CID spectra that the different reactions do lead to different combinations of protonated isomers of ferrocene, which in two of the studied systems also vary with temperature. The question arises as to how to recognise the different isomers. This can be rationalised in terms of the energy changes and the molecular contortions required to reach the different decomposition channels for each isomer.

Identification of isomers: ring-protonated ferrocene, 1c

The CID spectrum of ferrocene protonated by NH_4^+ shows very little H loss, whereas that protonated by *t*-$C_4H_9^+$ at high temperature shows almost exclusive H loss, a process that was found to be very efficient. Clearly, these two systems populate entirely different isomers. According to theory, **1a** and **1b** are the most stable forms, and are close in energy.[4] The energy of **1c** is significantly higher.[5] Experimentally, the proton affinity of ammonia is only 10 kJ mol^{-1} lower than that of ferrocene which is insufficient to populate **1c**.

In **1c** the ring to which the proton is attached adopts a structure very similar to ionized cyclopentadiene.[5] The CID spectrum of *c*-$C_5H_6^+$ was therefore investigated, using the charge-transfer reaction (5) to create the parent ion. This spectrum, shown in Figure 5, is indeed dominated by loss of H, which was found to be independent of reaction temperature and pressure. In the case of both parent ions, *c*-$C_5H_6^+$ and $FeCp_2H^+$ (ring-protonated), H loss is not only the simplest process (and therefore most entropically favoured), but also the least endothermic.[26] In addition, when the proton is attached to the topside of a ferrocene ring, not only is the extra H atom more exposed, but also the net energy to break this σ bonded H atom is considerably lowered because of the higher energy of the ring-protonated form **1c**. Conversely, in the metal-protonated and agostic forms, **1a** and **1b**, the labile H atom is both less conveniently placed for direct interaction during the collision, and requires more energy to bring it into the correct alignment for ejection from the collisionally activated ion. Ejection of H is therefore much more difficult, as shown by the very small H loss peak when ammonia is the protonating gas. Hence, we conclude that at high temperature t-$C_4H_9^+$ mainly populates **1c**, which readily ejects H during CID. At low temperatures the site of protonation changes, as discussed below.

$$Ar^+ + c\text{-}C_5H_6 \rightarrow Ar + c\text{-}C_5H_6^+ \qquad (5)$$

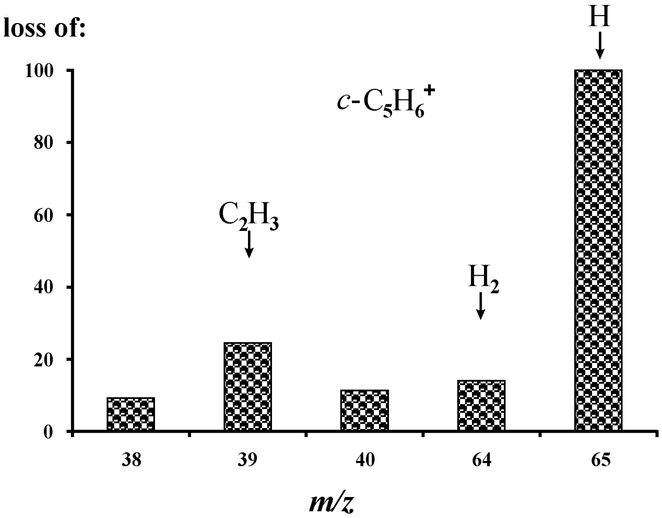

Figure 5. CID spectrum of ionized cyclopentadiene formed in argon, shown as normalized ion intensity of peaks ≥ 5% of the most abundant; the gas mixture was c-C_5H_6 in Ar in the ratio 1 : 160, pressure: 1 Torr, temperature: 465 K.

Identification of isomers: the metal-protonated (1a) and agostic forms (1b)

The ammonia experiments show that it is **1a** and **1b** that are predominantly responsible for the CID peaks at *m/z* 129 (***neutral loss***: FeH_2) and 121 (***nl***: c-C_5H_6). The energy required to reach the FeH_2 loss channel is much greater than that for c-C_5H_6 loss (Table 2). Nevertheless, at 270 K the *m/z* 129 peak in Figure 3c is 60% of the *m/z* 121 peak. The difference in the relative probabilities for these two processes occurring in each of the isomers will be determined mainly by the degree of rearrangement required to reach the relevant dissociation channel from the starting geometry. Clearly, the geometry of **1b** is already very close to that required for loss of c-C_5H_6. Furthermore, in **1a** the two rings are slightly more tilted towards each other[4] and away from the hydrogen atom attached to iron, which will favour the transition state geometry required for the fusion of the two rings to form $C_{10}H_9^+$ (*m/z* 129) when FeH_2 is ejected. We infer,[27] therefore, that in Figure 3(c) the greater relative loss of FeH_2, compared to the systems of Figures 3(a) and 3(b), indicates a significantly higher population of **1a** relative to **1b**, than in the other systems. This is consistent with **1a** as the most stable form of the isomers.

Protonation in the methane system

The cyclopentadienyl rings in ferrocene carry a net negative charge.[5] In addition, the iron atom is buried between the two rings of $FeCp_2$, making it relatively inaccessible. By *exo* attack, an electrophile will not only have greater access, but this will also be favoured by the electrostatic forces during the approach and formation of the ion-molecule complex. Since the energy carried by reagent ions in methane is well in excess of that required to populate all three isomers, a proton is easily deposited onto the ring, and the reaction is therefore expected to be fast. The transferred proton will also be very mobile initially, because of the exothermicity of the process, making its transfer into the agostic position also relatively efficient; not so transfer to the metal atom, however. The relatively small FeH_2 loss in Figure 3(a) demonstrates this point. Our observations on this system are therefore very similar to that reported by Hop and McMahon,[18] despite the quite different instruments used. The spectrum obtained therefore shows that both **1b** and **1c** are formed, but relatively little **1a**.

It is interesting that the methane-based CID spectrum showed no reaction temperature dependence, whilst the other two systems did. This tells us that the energy/entropy barriers between the different isomers are large enough that thermally induced interconversion between the isomers does not occur over the timescale of these reactions (the average lifetimes of ions in the chemical ionization reactor are[21] in the range of 10^{-4} to 10^{-3} s). The temperature dependences observed for the isobutane and ammonia systems are, therefore, the result of factors specific to the reaction chemistry of those systems.[28]

The t-$C_4H_9^+$ / $FeCp_2$ reaction

The iron atom in $FeCp_2$ is relatively inaccessible to direct attack by a large cation such as t-$C_4H_9^+$ (see Figure 7 below). As discussed above, under thermal conditions in the source, the approaching electrophile will in any case naturally tend to dock with one of the rings in the *exo* position, to form an ion-molecule complex in the first instance. In this system, asymmetric charge transfer (6) is near-resonant, and $FeCp_2^+$ (*m/z* 186) is therefore an important product of reaction, in addition to proton transfer (7), depending on the conditions, as is shown in Figure 2(b). In reaction (7), the lowest energy channel would involve rearrangement in the ion-molecule complex by migration of one of the protons from the t-$C_4H_9^+$ group and the formation of isobutene, which is then carried by rotational motion away from the complex. The complex itself also rearranges to a stable form, to make the adduct ion observed at *m/z* 243 (= 186 + 57) in Figure 2(b). The relative abundance of this ion in the spectrum was observed to increase with increasing temperature.

$$t\text{-}C_4H_9^+ + FeCp_2 \leftrightarrow (FeCp_2 \cdot t\text{-}C_4H_9)^+ \rightarrow t\text{-}C_4H_9 + FeCp_2^+ \quad (\Delta H = +3\ \text{kJ mol}^{-1})^{24} \qquad (\mathbf{6})$$

$$t\text{-}C_4H_9^+ + FeCp_2 \leftrightarrow (FeCp_2 \cdot t\text{-}C_4H_9)^+ \rightarrow i\text{-}C_4H_8 + FeCp_2H^+ \quad (\Delta H = -62\ \text{kJ mol}^{-1})^{13} \qquad (\mathbf{7})$$

Ion-molecule complexes are electrostatically bound and, because of the relatively weak bonding, are usually more stable at low temperatures. The increased abundance of the adduct (*m/z* 243) at higher temperatures is therefore indicative of further intramolecular reaction. This, together with the preference for the formation of **1c** at higher temperature, as discussed earlier and shown by Figure 3(b), suggests that a temperature induced change to the structure of the complex (*m/z* 243) occurs which favours *exo* ring protonation. This prompted us to measure the CID spectrum of the adduct (*m/z* 243) at different temperatures, as shown Figure 6. The result showed that at low temperatures the adduct gives loss of H and C_4H_9, but the high temperature CID gives loss of H_2 and C_4H_9, with the efficiency of decomposition increased two-fold over the temperature range studied.

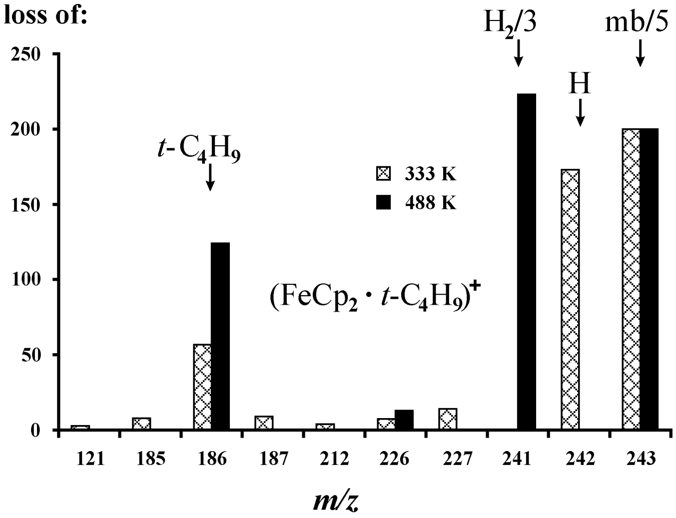

Figure 6. CID spectra of the ferrocene / *tert*-butyl adduct ion (*m/z* = 243) formed in isobutane at low and high reaction gas temperatures; pressure: 1 Torr; gas mixture same as Figure 3(b); mb: main (i.e. parent ion) beam.

In the complex, the simplest process is for the $t\text{-}C_4H_9^+$ group to become attached as a σ-bonded adduct to one of the carbon atoms, forming an alkylated cyclopentadiene ring (**2a** in Figure 7). This is the same type of complex as was suggested for the intermediate in the Friedel–Crafts acylation of ferrocene.[1] In CID, this complex would most easily lose either the H atom or the $t\text{-}C_4H_9$ group from the sp^3 hybridized carbon atom in reactions (8a) and (8b), leaving behind ionized *tert*-butyl ferrocene or ionized ferrocene respectively. In the proton transfer channel (7), rearrangement is required to enable formation of isobutene, but which then has the potential to form a π-complex between the double bond of the isobutene, the proton, and the π-system of a

$$\textit{CID} \qquad \sigma\text{-complex} \rightarrow (FeCp \cdot C_5H_4 \cdot t\text{-}C_4H_9)^+ + H \qquad \textbf{(8a)}$$

$$\textit{CID} \qquad \sigma\text{-complex} \rightarrow FeCp_2^+ + t\text{-}C_4H_9 \qquad \textbf{(8b)}$$

$$\textit{CID} \qquad \pi\text{-complex} \rightarrow (\mathrm{FeCp} \cdot \mathrm{C_5H_5} \cdot \mathrm{C_4H_7})^+ + \mathrm{H_2} \qquad (\mathbf{9a})$$

$$\textit{CID} \qquad \pi\text{-complex} \rightarrow \mathrm{FeCp_2}^+ + t\text{-}\mathrm{C_4H_9} \qquad (\mathbf{9b})$$

ferrocene ring, shown as **2b** in Figure 7. The proton in that complex would be ideally positioned for transfer to the ring edge, the protonation site favoured in this reaction system. During CID of **2b**, this proton is also well placed for easy elimination of H_2 as isobutene 'condenses' with the ring, to form ionized isobutenyl ferrocene, reaction (9a); this is the simplest chemical process envisaged to give the ion at *m/z* 241. The loss of H_2 during CID from the heated adduct (*m/z* 243) is seen to be a very efficient process, hence it is inferred that the changing structure of the adduct caused by the increase in temperature, is from a σ- to a π-complex, i.e. **2a** → **2b**.

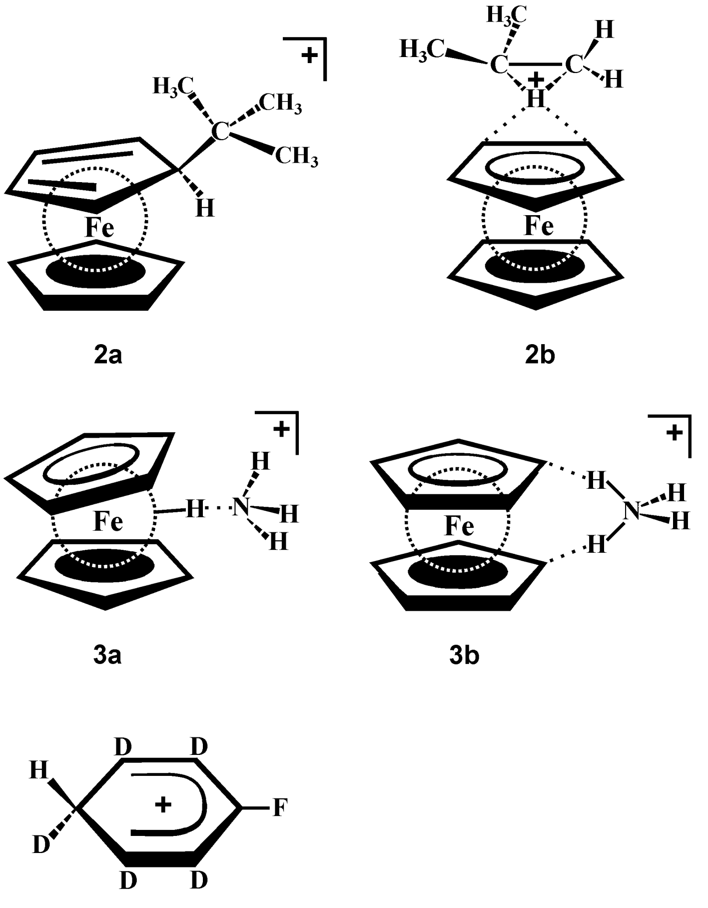

2a **2b**

3a **3b**

4

Figure 7. Postulated structures involving complexes of t-$C_4H_9^+$ (**2a** and **2b)** and NH_4^+ (**3a** and **3b**) with ferrocene, and the structure **4** of protonated C_6D_5F.[19]

The suggested overall reaction scheme of the relevant processes occurring in the isobutane gas mixture is therefore given by (10) to (14).

$$FeCp_2 + t\text{-}C_4H_9^+ \rightleftharpoons (FeCp_2 \cdot t\text{-}C_4H_9)^+_{\text{ion-molecule complex}} \qquad (\mathbf{10})$$

$$(FeCp_2 \cdot t\text{-}C_4H_9)^+_{\text{ion-molecule complex}} \rightleftharpoons (FeCp_2 \cdot t\text{-}C_4H_9)^{+*}_{\sigma\text{-complex}} \qquad (\mathbf{11})$$

$$(FeCp_2 \cdot C_4H_9^+)^*_{\sigma\text{-complex}}\ \mathbf{2a} \rightleftharpoons (FeCp_2 \cdot H^+ \cdot C_4H_8)^*_{\pi\text{-complex}}\ \mathbf{2b} \qquad (\mathbf{12})$$

$$(FeCp_2 \cdot C_4H_9)^{+*}_{\sigma\text{-complex}}\ \mathbf{2a} \rightarrow FeCp_2H^+_{\text{mixed isomers}}\ (\mathbf{1a}, \mathbf{1b}, \mathbf{1c}) + C_4H_8 \qquad (\mathbf{13})$$

$$(FeCp_2 \cdot H^+ \cdot C_4H_8)^*_{\pi\text{-complex}}\ \mathbf{2b} \rightarrow FeCp_2H^+_{\text{ring-protonated}}\ \mathbf{1c} + C_4H_8 \qquad (\mathbf{14})$$

The temperature dependence of the CID spectrum of the adduct ion therefore clearly demonstrates two points: (i) there are at least two isomers of the complex; and (ii) the low temperature complex is more tightly bound than the higher temperature structure, because the CID efficiency of the latter increases significantly. Since the isomers of $FeCp_2H^+$ do not interconvert over the timescale of the experiment (see earlier), the relative populations of **1b** and **1c**, as reflected by the c-C_5H_6 and H loss peaks in Figure 3(b) are probably determined by the relative populations of their precursors formed in reactions (13) and (14).

The NH_4^+ / $FeCp_2$ reaction

The loosely bound ion-molecule complex $(FeCp_2 \cdot NH_4)^+$ is not sufficiently stable to survive the journey through the mass spectrometer, hence a peak at *m/z* (186 + 18) was not detected in the chemical ionization spectrum, Figure 2(c), even at low temperature. However, this species was detected with high intensity decomposing in the accelerating region, giving a high background signal at *m/z* 186 in the B/E linked scan spectrum of the protonated ferrocene at *m/z* 187 (see experimental section).

Although initially, NH_4^+ will be drawn by electrostatic forces towards one of the rings, it carries insufficient energy to protonate the ring. To get to the right conformation for proton transfer, the ammonium ion must move, in the complex, into an *endo* position relative to ferrocene, in order to deposit the proton either directly onto the iron atom or up into the underside of the ring, to make the agostic form. This entropic restriction is, probably, what makes it a relatively slow reaction, even though it is slightly exothermic. Two different conformations are required in the two reaction channels (15) and (16). NH_4^+ is of the right size and structure to straddle across the two rings (**3b**), from which configuration ready transfer into the agostic position could be accomplished easily on either ring (see Figure 7). To get into the correct conformation for transfer to the metal atom, further rearrangement would have to occur as the rings tilt, allowing the ammonium ion to penetrate further, and twist to form a proton bound complex **3a** between the iron atom and the ammonia leaving group.

$$NH_4^+ + FeCp_2 \rightleftharpoons (NH_4 \cdot FeCp_2)^+\ \mathbf{3a} \rightarrow \mathbf{1a} \qquad (\mathbf{15})$$

$$NH_4^+ + FeCp_2 \rightleftharpoons (NH_4 \cdot FeCp_2)^+ \mathbf{3b} \rightarrow \mathbf{1b} \qquad (\mathbf{16})$$

As discussed above, thermally induced interconversion between the $FeCp_2H^+$ isomers themselves does not occur on a timescale fast enough to be observed by our experiments. The increased iron atom protonation at the lowest temperatures, shown by the CID spectrum in Figure 3(c), must therefore occur by intermolecular exchange, involving NH_3. This is supported by the results of the deuterium exchange experiments conducted previously by others. Using an ICR technique,[18,29] multiple exchanges were observed to occur between $Fe(C_5D_5)_2H^+$ and NH_3; this is in contrast to the highly exothermic reaction with D_3O^+ (discussed below), which involves only one exchange.[9]

Whilst the isomer composition is dependent on temperature, it is independent of both total reaction pressure and the partial pressure of $FeCp_2$. This effect, therefore, must reflect a steady state between different forms of the $(NH_4 \cdot FeCp_2)^+$ ion-molecule complex, in a similar way to the complexes formed in the isobutane system.

Isotope exchange and scrambling experiments

As evidence of iron atom protonation, Meot-Ner[9] conducted deuteration experiments in a reactor similar to ours, using D_3O^+ in N_2; there is more than enough energy in this reaction to transfer D^+ to the ring. However, only one D^+ was transferred to ferrocene, and it was argued that thermo-neutral hydrogen exchange with equivalent ring hydrogens between the ionic and neutral collision partners should have been expected, leading to mixed isotope products, by analogy with the benzene reaction,[30] and that therefore the D^+ must have transferred to a unique site. On the other hand, CID spectra of $FeCp_2D^+$, also formed from D_3O^+ (but in methane), showed[18] substantial loss of H and D, a strong indicator of ring protonation, in agreement with our findings. The very high H compared with D loss was interpreted[18] as evidence that the transferred atom was highly mobile. This is not necessarily the case, however, as we have sometimes found, such effects can be due to a very large isotope effect.[21]

In CID experiments, it is often difficult to distinguish between isotope scrambling in the parent ion, thermally induced by processes in the ion-molecule reactor, and that induced by the high energy collisional activation process, prior to its subsequent decomposition in the mass spectrometer. The only certain result is when scrambling does not occur. We therefore studied deuteration by $(C_6D_5F)H^+$ in methane, reaction (17). This system gave almost equal amounts of protonated and deuterated ferrocene, as shown in Figure 2(d). This was as expected because of the structure[19] of $(C_6D_5F)H^+$ (**4** in Figure 7), from which H or D atom exchange is equally probable. Protonation by CH_5^+ or $C_2H_5^+$ is also a possibility, but this does not impinge on the deuterated ferrocene. The CID spectrum of the produced deuterated ferrocene is shown in Figure 9. The CID gave fragments indicating all three sites of protonation and did not change with temperature or pressure, as was also observed for the methane system.

$$(C_6D_5F)H^+ + FeCp_2 \rightarrow C_6D_4HF + FeCp_2D^+ \quad (\Delta H_{reaction} = -108\ kJ\ mol^{-1})^{13} \qquad (\mathbf{17})$$

The signal for H and D loss, whilst either larger or at least a similar probability to the other major peaks, was small on top of a large background signal at this point of the B/E scanning plane (see the experiment section). The noise on this much larger background signal, therefore, made it impossible to obtain a reliable value for the H to D loss intensity ratio.

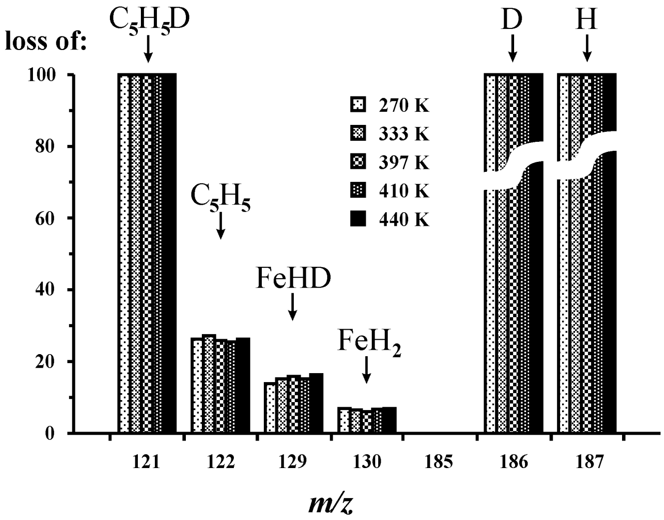

Figure 9. The CID spectrum of $FeCp_2D^+$ formed in reaction (17) as a function of temperature; p= 1 Torr; the reagent gas mix was $FeCp_2$: C_6D_5F : CH_4 in the ratio 1 : 10 : 3333. The break in the D and H loss peaks indicate that these could not be measured accurately (see text).

On the other hand, reproducible isotope ratios were obtained for the other fragments. Thus, the ratio for FeHD compared to FeH_2 loss is 2 : 1 which is 9 times higher than if complete scrambling of D amongst all the H atoms had occurred (giving a statistical ratio of 0.22 : 1, or 0.5 : 1 if the H atoms of only one of the Cp rings was involved). This indicates direct deuteration of the iron atom, and although exchange with the ring hydrogens probably does occur, it is not efficient. The ratio of *c*-C_5H_5D to *c*-C_5H_6 loss is 4 : 1 compared with the expected statistical distribution of 1.2 : 1. This indicates that D^+, transferred into the agostic position, also tends to stay in this position, with relatively little thermally induced scrambling or self-exchange, in good agreement with Meot-Ner's experiments.[9] This also concurs with the lack of any temperature dependence in the CID spectrum, which confirms that interconversion of isomers did not occur in the ion source over the timescale of our experiments.

The energy of protonated ferrocene isomers

The proton affinity difference between isobutene and ferrocene is[12] 62 kJ mol^{-1}. Furthermore, *t*-$C_4H_9^+$ readily protonates on the ring, therefore the energy of **1c** is ≤ 62 kJ mol^{-1} above the lowest energy isomer. Kebarle et al.[12] deduced a value of approx. 42 kJ mol^{-1} from kinetic studies. These estimates are well below the 176 kJ mol^{-1} predicted at the highest levels of MO theory.[5]

The metal-protonated **1a** and agostic **1b** isomers are clearly close in energy, because both are formed from the reaction with NH_4^+. This brackets their free energies within 10 kJ mol^{-1} of each other. The fact that the metal-protonated isomer **1a** becomes more populated at the lowest of the explored temperatures suggests that it is the lowest energy form.

Conclusions

By studying the gas phase chemistry of ferrocene protonation using high energy CID mass spectrometry, it is possible to identify and follow the changes in isomer populations. Experimental evidence for the stable existence of all three theoretically postulated isomers of $FeCp_2H^+$ has been obtained. Specific isomer populations have been shown to depend on the nature of the protonating agent and the reaction conditions. The results indicate that theoretical calculations do not allow accurate prediction of the correct order of stability for the protonated ferrocene isomers. The most stable isomer, inferred from the CID behaviour, appears to be the metal-protonated form. This does agree with experimental findings in solution,[7a] and it is < 10 kJ mol^{-1} lower than the agostic form. The ring-protonated structure has an energy which is >10, but ≤ 62 kJ mol^{-1} above the lowest energy form. This concurs with the observations by Kebarle et al.[12] There is an energy/entropy barrier between each of the isomers that prevents easy intramolecular thermal isomerization in the gas phase over the 10^{-3} s timescale and at pressures <5 Torr.

The t-$C_4H_9^+$ ion forms an intermediate complex with ferrocene, strong enough to be studied using high energy CID mass spectrometry, its structure changing with temperature. The low temperature structure is probably a ring edge-bound σ-complex, from which all three isomers of protonated ferrocene may be populated; but at high temperatures it changes, most likely to a π-π complex, which almost exclusively populates the ring-protonated form of ferrocene. The complex of ferrocene with NH_4^+ is metastable, and it too appears to alternate between different configurations, one of which leads to the agostic form and the other to the metal-protonated isomer of ferrocene, depending on the temperature.

Experimental Section

The experiments were carried out using a 'high pressure' ion-molecule reaction source attached to a mass spectrometer system, previously modified and described in detail elsewhere.[31] The gaseous reaction mixtures were pre-mixed in a heated gas storage bulb, by injection of a solution of ferrocene in toluene or perdeuterated fluorobenzene, with the molar ratio of ca. 1 : 10, directly into the reagent bath gas (e.g. methane). A typical gas mixture was ferrocene, toluene and methane in the ratio of 1 : 10 : 3333. The ratio of ferrocene to toluene was accurate to better than 0.5%, whilst the liquid vapour to bath gas mix was accurate to better than 3%. The mixture was allowed to flow continuously into the reactor, maintained at a constant pressure by an automatic control valve and pressure transducer arrangement. The temperature, measured to within ± 2°, could be varied between –100 and +400 °C and the source pressure up to 4 Torr, measured to within ± 0.02 Torr. The actual temperature range used was limited by the chemistry of the reagents and the intensity of the generated ion beam, sufficient to carry out CID mass spectrometry.

Reactant and product ions drifting through the very small ion exit aperture into a differentially pumped mass spectrometer ion beam accelerating region were accelerated to a beam energy of 6 keV. The CID spectrum of the ion of interest was monitored using the technique of "Constant B/E Linked Scanning", as before.[19] N_2 was used as the collision gas at a pressure sufficient to attenuate the main beam by 30 to 40%. CID peak intensities were recorded by linked scanning of the magnetic field (strength B) and electrostatic analyser (field E), whilst maintaining a constant B/E ratio. The full mass spectrum was collected by continuous automated scanning in the usual way. However, quantitative peak height ratios were measured by manual tuning, individually, onto the selected fragment ion peaks of interest, and recording the collector current of the beam at the top of the peak. This cautious method was used to ensure accurate tuning to find the top of the peak, which was not necessarily in its exact theoretical position because of translational energy loss in the collision. For this study, the long-term reproducibility for peak height ratios was found to fall within the limits of ± 5%.

Whilst the bulk of ions reaching the detector during the B/E linked scan are usually created by the collisional activation of the selected parent ion, it will also pick up: (i) the products of excited parent ions decomposing in a unimolecular fashion; (ii) the products of collision with the background gas; and (iii) ions from other processes occurring in the accelerating region of the instrument, which happen to come into focus at the same point in the B,E scanning plane.[32] The ions picked up in (i) and (ii) do not affect the interpretation of the results since they are still representative of the ion of interest. However, ions from (iii) can create a serious ambiguity, unless the effect is measured and taken into account; then it can sometimes itself be of value in interpreting the data. A background spectrum was, therefore, always obtained by running the spectrum in the absence of collision gas and making an appropriate correction[33] to the CID spectrum. Thus any contributions from (i), (ii) or (iii) are removed from the spectrum. In general, CID peaks were in the region between 0.1 and 4% of the main beam (parent ion) intensity. Background intensities were usually less than 10% of the CID peak intensity, except in some instances where the fragment ion resulted from loss of H or H_2.

The ^{13}C isotope of ferrocene is isobaric with $FeCp_2H^+$, and was found to contribute, usually, less than 1%, but at worst, no more than 3% to any peak used in the analysis of the CID spectra, and so did not pose a problem.[34]

Research grade gases from BOC (methane), BDH (isobutane) and Air Products (NH_3) were used throughout the study; ferrocene and other chemicals, obtained from Aldrich, were ≥ 99% pure and used as received.

“Interfering” metastable decompositions

Decompositions which contribute to (iii), above, must occur from ion adducts which are higher in mass than the parent ion of interest. Such ions, occurring during this study, were $(FeCp_2 \cdot t\text{-}C_4H_9)^+$, $(NH_4 \cdot FeCp_2)^+$ and $(C_6D_5F \cdot FeCp_2)H^+$ formed in the source by reactions (18), (20) and (22) respectively.

$$t\text{-}C_4H_9^+ + FeCp_2 \rightarrow (FeCp_2 \cdot t\text{-}C_4H_9)^{+*} \qquad \textbf{(18)}$$

$$\textit{Unimol.} \qquad (FeCp_2 \cdot t\text{-}C_4H_9)^{+*} \rightarrow FeCp_2^+ \ (m/z\ 186) + t\text{-}C_4H_9 \qquad \textbf{(19)}$$

$$NH_4^+ + FeCp_2 \rightarrow (NH_4 \cdot FeCp_2)^{+*} \qquad \textbf{(20)}$$

$$\textit{Unimol.} \qquad (NH_4 \cdot FeCp_2)^{+*} \rightarrow FeCp_2H^+ \ (m/z\ 187) + NH_3 \qquad \textbf{(21)}$$

$$(C_6D_5F)H^+ + FeCp_2 \rightarrow (C_6D_5F \cdot FeCp_2)H^{+*} \qquad \textbf{(22)}$$

$$\textit{Unimol.} \qquad (C_6D_5F \cdot FeCp_2)H^{+*} \rightarrow FeCp_2H^+ \ (m/z\ 187) + C_6D_5F \qquad \textbf{(23)}$$

$$\textit{Unimol.} \qquad (C_6D_5F \cdot FeCp_2)H^{+*} \rightarrow FeCp_2D^+ \ (m/z\ 188) + C_6HD_4F \qquad \textbf{(24)}$$

All are metastable, i.e. they survive long enough to enter the accelerating region, but decompose spontaneously as they pass through the mass spectrometer. These ions were found to decompose efficiently by unimolecular reactions (19), (21) and (23,24) in the accelerating region, close to the ion source. These processes are easily determined by mapping the B,E plane[32] and following the decomposition ‘trail’ which connects parent ions and fragments. The $FeCp_2^+$ product formed from reaction (4) at a particular point in the accelerating region has the same focusing conditions as $FeCp_2^+$ formed by reaction (1) in the first field free region. The B/E linked scan is a low resolution technique, and the decomposition trails for reactions (6) and (8) in the accelerating region pass very close to the decomposition trail for the loss of H and D from $FeCp_2D^+$ in the first field free region. Due to the very high intensities involved, they contribute significantly to the background signal for those reactions because of adjacent peak overlap. The $(NH_4 \cdot FeCp_2)^+$ ion was not detectable in the standard mass spectrum, but it was readily identified by its decomposition trail.

Acknowledgements

We thank the EPSRC for a studentship (LJK).

References and Notes

[#] *At the time of the experiments the authors were in the Chemistry Dept., now since closed.*

1. Cunningham, A. F. *J. Am. Chem. Soc.* **1991**, *113*, 4864.
2. Mueller-Westerhoff, U. T.; Haas, T. J.; Swiegers, G. F.; Leipert, T. K. *J. Organomet. Chem.* **1994**, *472*, 229.
3. Bühl, M.; Grigoleit S. *Organometallics* **2005**, *24*, 1516.
4. Mayor-Lopéz, M. J.; Lüthi, H. P.; Koch, H.; Morgantini, P. Y.; Weber, J. *J. Chem. Phys.* **2000**, *113*, 8009.
5. McKee, M. L. *J. Am. Chem. Soc.* **1993**, *115*, 2818, and references therein.
6. In essence, definitions of '*exo*' and '*endo*' refer to the approach of the electrophile towards the exposed face of the cyclopentadienyl ring and the underside of the ring, respectively.
7. (a) Curphey, T. J.; Santer, J. O.; Rosenblum, M.; Richards, J. H. *J. Am. Chem. Soc.* **1960**, *82*, 5249 (using ^{1}H NMR evidence); (b) most recently – Karlsson, A.; Broo, A.; Ahlberg, P. *Can. J. Chem.* **1999**, *77*, 628.
8. Cunningham, A. F. *Organometallics* **1994**, *13*, 2480.
9. Meot-Ner, M. *J. Am. Chem. Soc.* **1989**, *111*, 2830.
10. Foster, M. S.; Beauchamp, J. L. *J. Am. Chem. Soc.* **1975**, *97*, 4814.
11. Kerber, R. C. In *Comprehensive Organometallic Chemistry II*; Vol. 7; Shriver, D. F.; Bruce, M. I., Vol. Eds.; Abel, E. W; Stone, F. G. A., Wilkinson, G., Eds., Pergamon: Oxford, 1995, p. 186 and references therein.
12. Ikonomou, M. G.; Sunner, J.; Kebarle, P. *J. Phys. Chem.* **1988**, *92*, 6308.
13. Hunter, E. P. L.; Lias, S. G. *J. Phys. Chem. Ref. Data* **1998**, *27*, 413.
14. Irigoras, A.; Mercero, J. M.; Silanes, I.; Ugalde, J. M. *J. Am. Chem. Soc.* **2001**, *123*, 5040.
15. Long, N. J., *Metallocenes. An Introduction to Sandwich Complexes*; Blackwell Science Ltd.: London, 1998, pp 137-138; Fey, N. *J. Chem. Technol. Biotechnol.* **1999**, *74*, 852.
16. Mayor-Lopéz, M. J.; Weber, J. *Chem. Phys. Lett.* **1996**, *281*, 226.
17. Allison, C. E.; Cramer, J. A.; Hop, C. E. C. A.; Szulejko, J. E.; McMahon, T. B. *J. Am. Chem. Soc.* **1991**, *113*, 4469.
18. Hop, C. E. C. A.; McMahon, T. B. *J. Am. Soc. Mass Spectrom.* **1994**, *5*, 274.
19. Mason, R. S.; Parry, A. J.; Milton, D. M. P. *J. Chem. Soc., Faraday Trans.* **1994**, *90*, 1373.
20. Mason, R. S.; Williams, C. M.; Anderson, P. D. J. *J. Chem. Soc., Chem. Comm.* **1995**, 1027.
21. Mason, R. S.; Anderson, P. D. J.; Williams, C. M. *J. Chem. Soc., Faraday Trans.* **1998**, *94*, 2549.
22. Mason, R. S.; Naylor, J. C. *J. Phys. Chem. A*, **1998**, *102*, 10090.
23. On average, the ions in this study experience > 80 collisions before leaving the ion source, and the reactor is field free, therefore most ions will be collisionally thermalized before they leave the source.

24. Based on data given in Lias, S. G.; Bartmess, J. E.; Liebman, J. F.; Holmes, J. L.; Levin, R. D.; Mallard, W. G. *J. Phys. Chem. Ref. Data*, **1988**, *17*, 1.
25. The NIST Chemistry WebBook, Mallard, W. G., Ed.; http://webbook.nst.gov/chemistry.
26. The loss of H from c-$C_5H_6^+$ requires about 327 kJ mol^{-1}, whilst loss of H from ring protonated ferrocene requires about 150 kJ mol^{-1}. The higher energy processes, representing breakup of the ring, seen for ionised cyclopentadiene are not prominent in the CID of ring protonated ferrocene, because the alternative decomposition pathways available to it are so much lower in energy.
27. Another possibility that should be considered is the changes in rotational energy of the ion prior to collisional activation.[22] Rotation of the two rings would inhibit the required migration of the H atom from Fe to one of those rings to form c-C_5H_6. The same is true for the formation of FeH_2 when an H atom must migrate off one of the rings onto Fe. In addition, a lower degree of internal rotation would also aid the fusion of the two rings to make $C_{10}H_9^+$ (*m/z* 129), the conjugate ion in the FeH_2 loss process. On these grounds we would also conclude that metal protonation is favoured at the lower temperature, since the ratio FeH_2 / c-C_5H_6 increases with decreasing temperature. However, the lack of any such temperature effect in Figure 3a indicates that internal rotation effects do not show up in these systems, and that the temperature induced change is caused by the external chemistry.
28. One critic has argued that the lack of temperature dependence in this system could be because the ion is still very excited at the point of CID, with an energy above the barrier to interconversion. However under our experimental conditions each ion endures an average of 80 collisions before it leaves the reactor. Most excess energy transferred due to the exothermicity of a reaction is dissipated within the first few collisions. Powerful evidence that this is not an issue is given by the fact that the spectra are independent of pressure and therefore independent of the number of collisions.
29. Hunt, D. F.; Sethi, S. K. *J. Am. Chem. Soc*. **1980**, *102*, 6953.
30. Ausloos, P.; Lias, S. G. *J. Am. Chem. Soc.* **1981**, *103*, 3641; Hunter, E. P.; Lias, S. G. *J. Phys. Chem.* **1982**, *86*, 2769.
31. Mason, R. S.; Parry, A. J. *J. Chem. Soc., Faraday Trans.* **1992**, *88*, 3331.
32. Mason, R. S.; Farncombe, M. J.; Jennings, K. R.; Scrivens, J. *Int. J. Mass Spectrom. Ion Phys.* **1982**, *44*, 507.
33. To obtain consistent results, the following procedure must be used. Let the background peak of the B/E linked scan signal at a particular point, say at an *m/z* value equivalent to F_2^+, be $I_{background}$. Let the total signal under CID conditions be I_{total}. Suppose that for the CID experiment the ion beam intensity of the parent ion, **M**H^+, is reduced to a fraction 0.6 of its original value due to scattering, then any ions within the beam including those created in the accelerating region will, to a first approximation, suffer a similar attenuation, and this must be corrected for when making the background correction. The true CID intensity is then given by $I_{corrected} = I_{total} - (I_{background} \times 0.6)$. This is especially important when the background is a significant fraction of the total. Once this procedure was adopted, we have had no trouble

in obtaining self-consistent and reproducible results, even where there was a very large background. If self-consistency and reproducibility is not achieved the data is rejected.

34. $Fe^{13}CC_9H_{10}^+$ is isobaric with $FeCp_2H^+$. However, its peak height is 11% of the $FeCp_2^+$ peak at *m/z* = 186 and, under the conditions of measurement the peak at *m/z* 186 was usually less than 30% of that at *m/z* 187. In addition, the CID of $FeCp_2^+$ was measured to be an order of magnitude less efficient than that of $FeCp_2H^+$. Therefore, even under the worst conditions of isobaric overlap, the interference contributed ≤ 3% to any of the peaks in all the CID spectra of $FeCp_2H^+$ obtained in this study.